

Traction Electrification of Heavy Off-Road Vehicle: Case Study of Backhoe Loader Operating in Backfill

Pedro H. A. de Oliveira*, Igor A. Pires***, Braz de J. C. Filho**, Anderson do Nascimento****, Thales A. C. Maia**

* Graduate Program in Electrical Engineering, Federal University of Minas Gerais, Belo Horizonte, Brazil (e-mail: pho.marconi@gmail.com)

**Department of Electrical Engineering, Federal University of Minas Gerais, Belo Horizonte, Brazil (e-mail: thalesmaiaufmg@gmail.com, braz.cardoso@ieee.org)

*** Department of Electronic Engineering, Federal University of Minas Gerais, Belo Horizonte, Brazil (e-mail: iap@ufmg.br)

**** CNH industrial (e-mail: anderson.nascimento@cnhind.com)

Abstract: The objective of this paper is to size the power required by the main powertrain components used to electrify a backhoe loader in order to meet the requirements demanded by an operating cycle called backfill. The backhoe loader is modelled based on the external forces acting on itself. The power sizing approach was inspired in a technique applicable to the on-road vehicle electrification. This technique was adapted to electrify a backhoe loader. The backhoe loader modelling and the power sizing were implemented in a script developed in MATLAB. The simulation results showed backhoe loader is not able to recover braking kinetic energy along the backfill. The results also showed that power minimization of the engine-generator set maximizes the capacities of power and energy of the electrical energy storage source.

Keywords: non-road mobile machinery (NRMM); backfill; series hybrid electric powertrain; backhoe loader; loading bucket; power sizing; traction motor; engine-generator set; and electrical energy storage source.

1. INTRODUCTION

Environmental protection government agencies are progressively restricting polluting gas emission levels from heavy off-road vehicles (Eur-Lex, 2016). The electrification of heavy off-road vehicles, also known as non-road mobile machinery (NRMM), becomes a popular alternative among manufacturers to comply with government regulations (Wu et al. 2020; Hiroki et al. 2016; Abdel-Baqi et al. 2013).

Backhoe loaders are compact and versatile NRMMs and are often employed in mining and construction activities. Backhoe loaders have demand growth forecast for the upcoming years (Persistence, 2018). Therefore, the academy and the industry research and develop electrified backhoe loaders (Mendes et. al 2019; John Deere 2021; Case 2020).

Vehicle development has been boosted by the model-based design technique (Smith et al. 2017). Certain types of model-based design such as the dynamic modelling (Wang et al. 2017) and the multi-stage modelling (Liukkonen 2013) are employed to predict behavior of many electrical and mechanical variables of NRMM hybrid electric powertrain design. These modellings allow to change designs before construct a prototype and also allow sizing of powertrain components by analyzing the electrical and mechanical variables. However, these models are time-consuming and present high implementation complexity because of high number of subsystems and high level of interaction between them.

This work aims to propose a simple and straightforward method to size power of the main powertrain components used in the backhoe loader electrification. This method ensures the backhoe loader powertrain is capable of meeting the performance requirements demanded by an application. It means powertrain will have power and energy enough to perform a selected operating cycle. The approach proposed in this work models a backhoe loader based on the external forces acting on itself along an operating cycle called backfill in this work. The main powertrain components are: motor, engine-generator set and electrical energy storage source. The method proposed in this work is not intended to replace model-based design techniques since they are used to simulate the powertrain behavior along the vehicle development phase.

This paper contributes with power sizing of the main powertrain components for backhoe loader electrification based on a modified technique applied initially to on-road vehicles. The technique was modified by regarding the hydraulic power demanded by the backhoe loader loading bucket. Section 2 introduces operating cycle and backhoe loader. Section 3 addresses the backhoe loader modelling and power sizing. Section 4 presents results and discussion of these results. Finally, section 5 presents the paper conclusions.

2. OPERATING CYCLE AND BACKHOE LOADER

NRMM electrification design requires a certain level of knowledge about the machine functioning and a deeper

knowledge about its operating cycle. Therefore, backhoe loader functioning and the operating cycle selected are addressed before the methodology.

2.1 Backfill

An operating cycle generally comprises vehicle speed data and road elevation over time. Although, complementary system variables can be included to the cycle (O’Keeke al. 2007). Oil pressure and flow in the backhoe loader hydraulic pump output, and the backhoe loader speed are parameters that were measured along the operating cycle called backfill in this paper. These parameters are used on the power sizing calculus.

The backfill is an operating cycle in which backhoe loader traction system is predominantly used. A backhoe loader uses its front bucket lowered and touching the ground to push the loosened earth pile towards an opened ditch in the backfill. Fig. 1 illustrates the backfill steps carried out by a backhoe loader. Fig. 1(a) shows a backhoe loader going toward earth pile and pushing earth into ditch. Fig. 1(b) shows backhoe loader returning to its initial position with front bucket raised. Fig. 1(c) shows the backhoe loader restarting the maneuverings done on Fig. 1(a).

The backhoe loader travels short distances along the backfill. The backhoe loader speed tends to be low and variable due to constant accelerations and decelerations. There is possibility to recover braking kinetic energy along decelerations to recharge energy storage source. Traction power must be at least negative to analyze braking kinetic energy recovery feasibility.

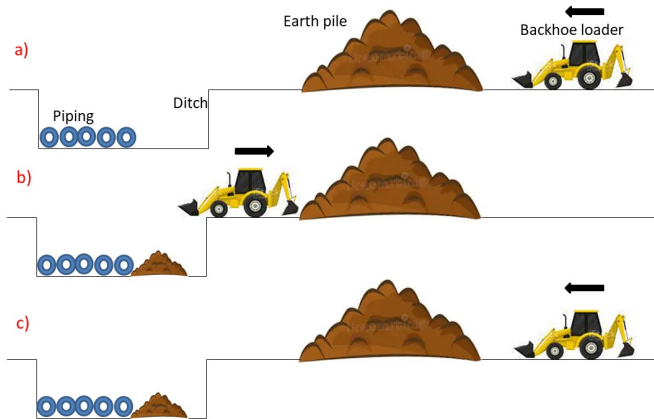


Fig. 1 Backfill stages: (a) backhoe loader advance; (b) return of backhoe loader; (c) restarting of backhoe loader advance.

2.2 Backhoe Loader

A backhoe loader performs two main types of activities: excavation and loading. The loading is performed along the backfill. A backhoe loader is divided into three main groups: tractor, loading bucket, and excavation shovel (see Fig. 2). The loading bucket and excavation shovel are generically called hydraulic implements.



Fig. 2 A backhoe loader divided into three main groups.

Fig. 3 illustrates a simplified hydromechanical schematic diagram that comprises the main powertrain components of a conventional backhoe loader. The hydraulic pump is mechanically connected to the internal combustion engine (ICE). Therefore, the oil from the hydraulic system circulates as long as the ICE is on. This topology feature decreases powertrain efficiency because hydraulic power is not transferred necessarily into effective work by the hydraulic implements.

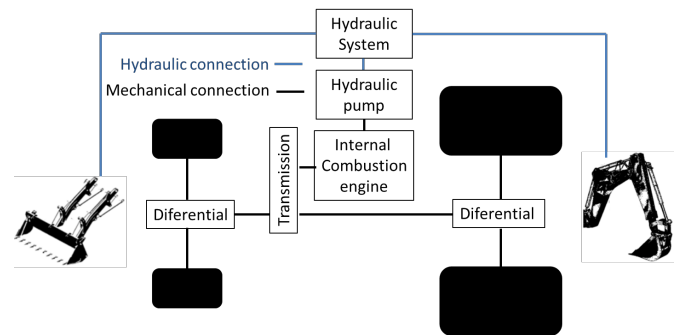


Fig. 3 Illustrative schematic diagram of a backhoe loader conventional powertrain.

One of the main electrification objectives is to increase powertrain efficiency. There are many topology options to electrify a powertrain, like battery electric, series hybrid electric, parallel hybrid electric, and series-parallel hybrid electric (Denton 2016). Battery electric powertrain is not considered in this work because a backhoe loader down time for the battery recharging is relatively high (Un-noor et al. 2021). Therefore, hybrid electric powertrains are the remaining topology options.

Series hybrid electric was the chosen topology (see Fig. 4). This architecture was selected basically due to powertrain internal room and engine operation requirements. A backhoe loader has limited internal room since it is a compact NRMM. The backhoe loader engine should probably work outside its maximum efficiency zone because of speed and torque values that can change a lot along the backfill. This is the ideal condition to employ the series hybrid electric topology (Kim et al. 2019).

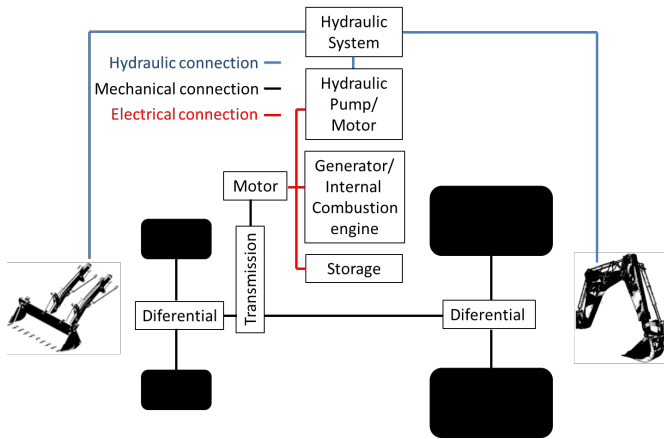


Fig. 4 Illustrative schematic diagram of the series hybrid electric powertrain chosen for this work.

3. METHODOLOGY

The backhoe loader modeling method applied in this work is based on the external resistance forces that are acting on a backhoe loader along the backfill. The backhoe loader equation parameters used in this work were estimated based on a commercial backhoe loader. The methodology applied in this paper was inspired on the power sizing technique of the main powertrain components for electrification of on-road vehicles proposed by Ehsani et al. (2018). Although, this technique was modified because a NRMM use its hydraulic implement during an operating cycle and the backhoe loader of this work use its loading bucket along the backfill.

3.1 Backhoe Loader Modeling

Model an on-road vehicle is basically to model the resistance forces (Mi et al 2017). The same concept could be applied to the backhoe loader modeling. But the resistance forces acting on the loading bucket are not applied to an on-road vehicle modeling. Thus, this technique must be modified in order to include the resistance force acting on the loading bucket. The external resistance forces acting on a backhoe loader can be represented in Fig. 5.

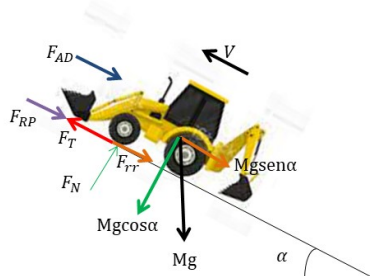


Fig. 5 Diagram of external resistance forces acting on a backhoe loader.

The traction force F_T required by a backhoe loader can be determined through the following equation (da Costa 2009):

$$F_T = F_{RR} + F_{AD} + F_G + F_A + F_{RP} \quad (1)$$

where F_{RR} is the rolling resistance force, F_{AD} is the aerodynamic drag force, F_G is the climbing resistance force that is null along the backfill, F_A is the acceleration force, and F_{RP} is the resistance force acting on a the loading bucket.

The rolling resistance force F_{RR} can be determined by the following equation:

$$F_{RR} = K.M.g.\cos(\alpha) \quad (2)$$

where K is the rolling resistance coefficient whose value estimated is 0.176, g is the gravity acceleration, e M is the vehicle mass whose value estimated is 7,462 kg. The vehicle mass value includes the additional weight of the main powertrain components used for the backhoe loader electrification which also includes an energy storage source.

The aerodynamic drag force F_{AD} can be determined by the following equation:

$$F_{AD} = \frac{1}{2}.\rho.A.C_D.V^2 \quad (3)$$

where ρ is the air volumetric density, A is the backhoe loader front area whose value is 6.46 m², C_D is the aerodynamic drag coefficient whose value is 0.45 and V is the backhoe loader speed.

The climbing resistance force F_G is determined by the following equation:

$$F_G = M.g.\sen(\alpha) \quad (4)$$

The acceleration force F_A can be determined by the following equation:

$$F_A = M.\delta.\frac{dV}{dt} \quad (5)$$

where $\frac{dV}{dt}$ is the acceleration and δ is the rotational inertia factor whose function is to transform rotational mass into translational one. The estimated rotational inertia factor value is 1.01.

The resistance force that act on the loading bucket F_{RP} along the backfill can be determined by the following equation (Zou et al. 2018):

$$F_{RP} = F_{x1} + F_{x2} + F_{x3} + F_{x4} \quad (6)$$

where F_{x1} is the resistance force to cut horizontally the loosened earth pile, F_{x2} is the loosened earth displacement resistance force inside the loading bucket, F_{x3} is the resistance force of friction between loosened earth and the loading bucket, and F_{x4} is the horizontal component of the friction resistance force between the loosened earth that goes

up and the internal face of the loading bucket. The Fig. 6 illustrates the resistance forces on the loading bucket along the backfill.

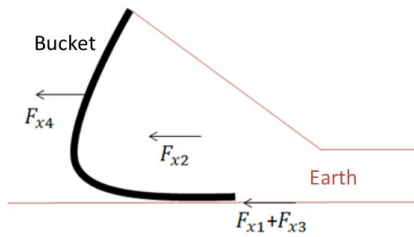


Fig. 6 Illustration of the diagram of resistance forces on a backhoe loader loading bucket along the backfill.

The resistance force to cut horizontally the loosened earth F_{x1} can be determined by the following equation:

$$F_{x1} = K_b \cdot B_c \cdot h \quad (7)$$

where K_b is the cutting resistance per area unit in Pa whose value is 45 kPa (Zou et al. 2018), B_c is the loading bucket width whose value is 1 m, and h is the earth layer height whose value estimated is 0.11 m.

The loosened earth displacement resistance force F_{x2} is determined by the following equation:

$$F_{x2} = \mu_2 \cdot \rho_T \cdot B_c \cdot \frac{(H-h)^2}{2 \cdot k_m \cdot tg(\phi)} \quad (8)$$

where μ_2 is the internal friction coefficient between the earth grains whose value is 0.5 (Zou et al. 2018), ρ_T is earth density whose value estimated is $1.73 \cdot 10^3 \text{ kg/m}^3$ - red latosol in medium textured field with T2 compaction level - (Beutler et al. 2005), H is the loading bucket height whose value is 0.42 m, K_m is the earth mass scale factor whose estimated value is 1.27 (Zou et al. 2017), ϕ is the repose angle between the loosened earth pile in front of the loading bucket and the earth layer to be removed (see Fig. 7) whose tangent estimated is 0.47.

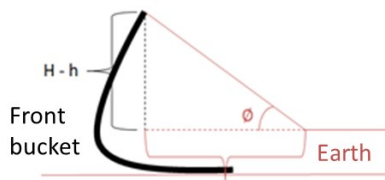


Fig. 7 Repose angle illustration.

The friction resistance force between the loosened earth to be removed and the loading bucket F_{x3} is determined by the following equation:

$$F_{x3} = K_y \cdot B_c \cdot x \cdot \mu_1 \quad (9)$$

where K_y is the resistance per pressure unit applied to the loading bucket moving into the loosened earth whose estimated value is 50 kPa (Zou et al. 2018), x is the contact area between the loading bucket and the ground whose value is 0.48 m², and μ_1 is the friction coefficient between the loading bucket and the ground whose estimated value is 0.4 (Stefanow et al. 2018).

The horizontal component from the friction resistance force between the loosened earth that goes up and the internal face from the loading bucket F_{x4} is determined by the following equation below:

$$F_{x4} = \mu_1 \cdot \rho_T \cdot B_c \cdot \frac{(H-h)^2}{2 \cdot k_m \cdot tg(\phi)} \cdot \cos^2(\xi) \quad (10)$$

where ξ is the loading bucket cutting angle whose value is 22°.

The backhoe loader modeling equations shown in this section were implemented in a MATLAB script to obtain the simulated traction force F_T .

3.2 Power Sizing of the Main Powertrain Components Used in the Backhoe Loader Electrification

Design the powertrain of an on-road vehicle means to ensure that the vehicle has the desired performance to run the selected driving cycle (Ehsani et al. 2018). It means that the powertrain needs to have power enough to run the driving cycle. This concept does not change radically when the designed vehicle is a NRMM. This work proposes to size the power required by the main powertrain components used to electrify a backhoe loader. The main components are: motor, engine-generator set, and energy storage source.

3.2.1 Traction Motor Power Sizing

The traction motor power sizing applied to the series hybrid electric on-road vehicle is the same of the battery electric on-road vehicle (Ehsani et al. 2018). This power sizing can be applied to the backhoe loader as well since its traction system is similar of the on-road vehicle. The traction motor power sizing regards three fundamental parameters: torque, rotating speed, and power. The traction motor torque can be obtained through the traction force F_T equation as expressed below:

$$F_T = \frac{T_m \cdot i_g \cdot i_0 \cdot \eta_t}{r_d} \quad (11)$$

where T_m is the traction motor torque, i_g is the gear ratio along backfill, i_0 is the final gear ratio (product between the differential and wheel hub gear ratios), η_t is the transmission efficiency whose value is 0.9, and r_d is the tire radius whose value is 0.66 m. Therefore, the traction motor torque T_m is determined by the following equation:

$$T_m = \frac{F_T \cdot r_d}{i_g \cdot i_0 \cdot \eta_t} \quad (12)$$

The traction motor rotating speed N_m can be obtained through the backhoe loader speed V that is determined by the following equation:

$$V = \frac{N_m \cdot r_d \cdot \pi}{i_g \cdot i_0 \cdot 30} \quad (13)$$

where N_m is the traction motor rotating speed in (rpm) that is determined by the following equation:

$$N_m = \frac{V \cdot i_g \cdot i_0 \cdot 30}{r_d \cdot \pi} \quad (14)$$

Finally, the traction motor power P_m is determined by the following equation:

$$P_m = T_m \cdot N_m \cdot \frac{\pi}{30} \quad (15)$$

The equations shown in this section were implemented in a MATLAB script to obtain traction motor torque, rotating speed and power of the traction motor.

3.2.2 Engine-Generator Set Power Sizing

The engine-generator set power sizing applied to a NRMM differs from an on-road vehicle due to the hydraulic implements. Therefore, the engine-generator set power sizing applied to a backhoe loader must consider the hydraulic power demanded by the hydraulic implements as well as the conventional NRMM does (Liu et al. 2017). The engine-generator set power sizing is based on the average power required by an operating cycle selected. There are two different operating cycles that this work regards to size power for the engine-generator set: transit on a flat road and the backfill.

The backhoe loader develops constant speed, the hydraulic implements are not used, and the energy storage source does not supply power along the transit on a flat road. Thus, the average power for constant speed P_{vc} on a flat road is determined by the following equation (Ehsani et al. 2018):

$$P_{vc} = \frac{P_{RR} + P_{AD_{vc}}}{1000 \cdot \eta_t \cdot \eta_m} = \frac{K \cdot M \cdot g \cdot V + P_{AD_{vc}}}{1000 \cdot \eta_t \cdot \eta_m} \quad (16)$$

where P_{RR} is the rolling resistance power, $P_{AD_{vc}}$ is the aerodynamic drag power for the backhoe loader maximum constant speed value of 40 km/h, and η_m is the traction motor efficiency whose estimated value is 0.90.

The backhoe loader presents variable speed due to often accelerations and decelerations, loading bucket intermittent usage, and energy storage source usage along the backfill.

Thus, the average power for variable speed (P_{vv}) on the backfill is determined by the following equation:

$$P_{vv} = \frac{1}{T} \int_0^T \frac{(P_{RR} + P_{AD_{vv}} + P_A + P_{RP})}{1000 \cdot \eta_t \cdot \eta_m} \cdot dt + \frac{1}{T} \int_0^T \frac{P_{mh}}{\eta_{mh}} \cdot dt \quad (17)$$

where $P_{AD_{vv}}$ is the variable speed aerodynamic resistance power, P_A is the backhoe loader acceleration power, P_{RP} is the resistance power on the loading bucket, η_{mh} is the hydraulic pump-motor set efficiency whose value is 0.85 (Cassapa 2018), P_{mh} is the hydraulic pump-motor set power that is determined by the equation below (Cassapa 2018, 2018):

$$P_{mh} = \frac{\Delta p \cdot v}{600} \cdot \eta_{mh} = \frac{(\Delta p_{bp} \cdot v_{bp} + \Delta p_{bd} \cdot v_{bd})}{600} \cdot \eta_{mh} \quad (18)$$

where Δp and v are the pressure and flow of the hydraulic pump-motor set in (bar) and (l/min) respectively. The sub-indexes bp and bd are related to the main and steering outputs from the hydraulic pump-motor set.

The engine-generator set power $P_{e/g}$ should be greater than P_{vc} and P_{vv} . $P_{e/g}$ must be at least equal to the greater value between P_{vc} and P_{vv} . The average power supplied by the engine-generator set should be greater than the average power of the resistance loads to keep the backhoe loader energy storage source balanced along the backfill. Keep the electrical energy storage source balanced means to keep the state of charge between top and bottom limits. The energy storage source does not supply power along the transit on a flat road to avoid deep discharge.

The equations shown in this section were implemented in a MATLAB script to obtain the power required by the engine-generator set.

3.2.3 Power and Energy Sizing of the Energy Storage Source

The energy storage source used in the paper is also called Peak Power Source (PPS). The Acronym PPS is self-explanatory about the energy storage source function that is to supply the peak power values that are not supplied by the engine-generator set (Ehsani et al. 2018).

The PPS power sizing of an on-road vehicle is not the same of a NRMM due to the peak power demanded by the hydraulic implements. Thus, the PPS power P_{PPS} demanded by the backhoe loader is determined by the equation below:

$$P_{PPS} \geq \frac{P_{m,max}}{\eta_m} + \frac{P_{mh,max}}{\eta_{mh}} - P_{e/g} \quad (19)$$

where $P_{m,max}$ the motor peak power, $P_{mh,max}$ is the hydraulic pump-motor set peak power. If $P_{e/g}$ is sized to have

minimum power, its means $P_{e/g}$ is equal to P_{vc} or P_{vv} , P_{PPS} is sized to have maximum power by the analysis of (19).

The energy sizing must regard the operating cycle that does not present changes in energy. The transit on a flat road does not present energy variations. Therefore, the backfill is the operating cycle selected to the PPS energy sizing. The PPS energy E_{PPS} required by the backhoe loader is determined by the following equation:

$$E_{PPS} = \frac{\Delta E_{\max}}{SoC_{top} - SoC_{bott}} \quad (20)$$

where ΔE_{\max} is the maximum energy variation of the PPS that is equal to the difference between the maximum and minimum values of ΔE along the backfill, SoC_{top} is the state of charge top value which is 0.7, and SoC_{bott} is the state of charge bottom value which is 0.4 (Ehsani et al. 2018). The energy variation of the PPS ΔE is determined by the following equation:

$$\Delta E = \int P_{PPS,inst.} dt \quad (21)$$

where $P_{PPS,inst.}$ is the PPS instantaneous power that is determined by the equation below:

$$P_{PPS,inst.} = \frac{P_{m,max}}{\eta_m} + \frac{P_{mh,max}}{\eta_{mh}} - P_{e/g,inst.} \quad (22)$$

where $P_{e/g,inst.}$ is the engine-generator set instantaneous power that must be greater or equal to the backhoe loader instantaneous power along the backfill $P_{vv,inst.}$ whose equation is determined by:

$$P_{vv,inst.} = \frac{(P_{RR} + P_{AD_{vv}} + P_A + P_{RP})}{1000 \cdot \eta_t \cdot \eta_m} + \frac{P_{mh}}{\eta_{mh}} \quad (23)$$

The equations shown in this section were implemented in a MATLAB script to obtain the power and energy capacities demanded by the PPS.

5. RESULTS AND DISCUSSIONS

The backhoe loader traction force, speed, and traction power graphics can be seen in the Fig. 8. The backhoe loader presents low speed and often accelerations and decelerations along the backfill. Hence there is great variation in traction power whose values reach minimum of zero and maximum of 74.58 kW. The traction force also presents large variation. The graphics of traction force and power do not show negative values along the deceleration. Therefore, the backhoe loader should not recover braking kinetic energy along the backfill. The Fig. 9 reveals that the traction force would be negative during decelerations with null rolling resistance force. The blue line represents the difference

between the traction and rolling resistance forces while the green line represents just the rolling resistance force. It means that the braking kinetic energy recovery would be possible with null rolling resistance force. The high values of rolling resistance force are a consequence of the high value of rolling resistance coefficient (0.176). This is due to the type of floor and the backhoe loader high mass value (7,462 kg).

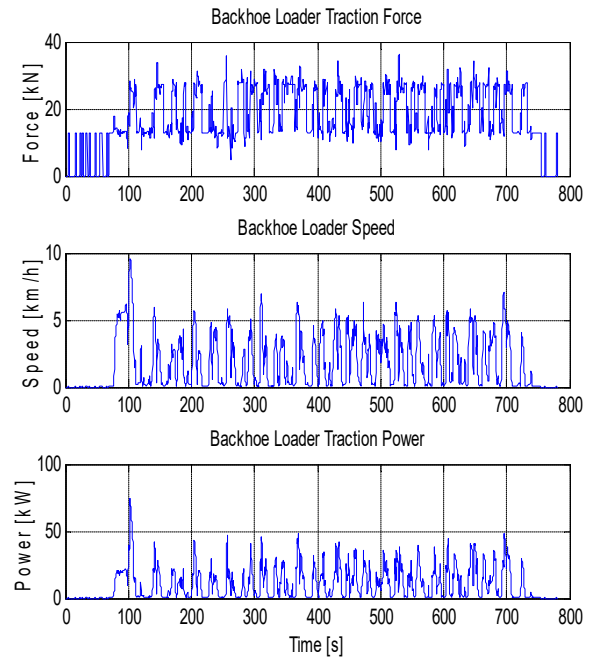


Fig. 8 Simulation of the traction force, backhoe loader speed, and traction power.

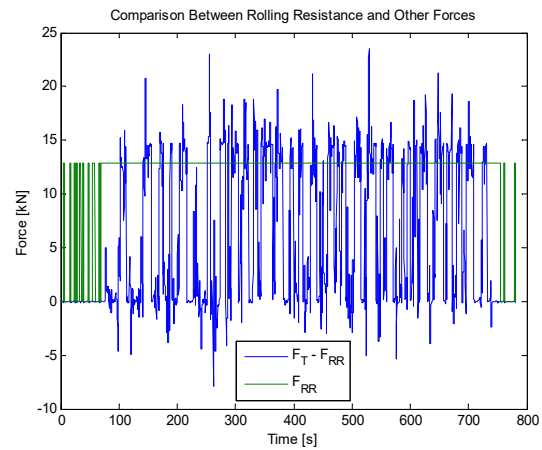


Fig. 9 Comparison between resistance forces without rolling resistance force and the rolling resistance force.

The torque, rotating speed, and power graphics of the traction motor are shown in the Fig. 10. Their curve profiles are quite similar when compared to the traction force, speed and traction power of the backhoe loader. The similarity between the curve profiles of the Fig. 8 and Fig. 10 were already expected. The torque and the rotating speed of the traction motor are proportional to the traction force and backhoe loader speed respectively according to (12) and (14). The

power sized for the traction motor (maximum value of 82.86 kW) differs of the backhoe loader traction power (maximum value of 74.58 kW). The difference between these two power values is due to losses in the backhoe loader transmission. This proposition can be confirmed multiplying the traction motor power by the transmission efficiency whose value is 0.9. The result is equal to the traction power value.

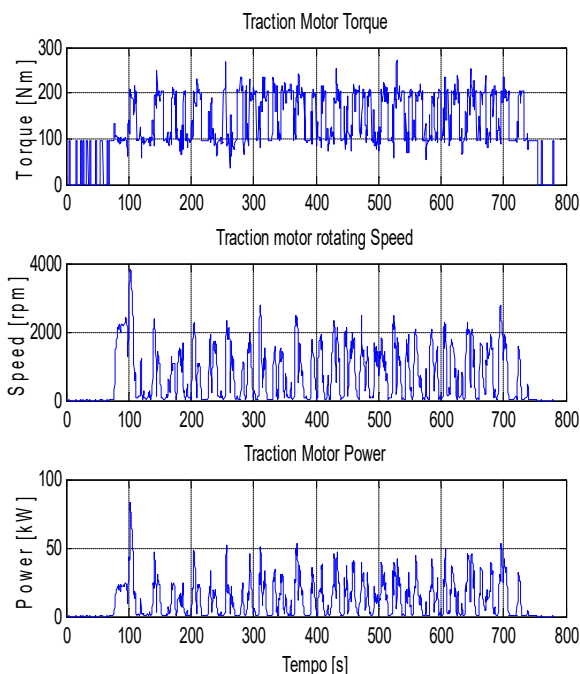


Fig. 10 Simulation of the torque, rotating speed, and power of the traction motor.

The average power value in constant speed (transit on a flat road) is 19.34 kW. The average power value in variable speed (the backfill) is just 13.10 kW. Therefore, the minimum average power value selected to the engine-generator set is 19.34 kW. This means that the PPS power and energy are maximized and their values are 78.14 kW and 61.02 kWh respectively. The low power value sized to the engine-generator set is offset by the high power and energy values sized to the PPS.

The power value sized to the engine-generator set is considerably lower than the power of a commercial backhoe loader engine. This means the backhoe loader electrified in this work has great potential to consume less fuel because the fuel instantaneous consumption is proportional to the engine power (Liu et al. 2017). Although, the PPS must to supply the power peaks required by the traction and hydraulic system and this could hinder the electrification financially. The application of a multi-criterion decision making (MCDM) method can aid the power sizing optimization and enable the electrification financially (Loganathan et al. 2021).

6. CONCLUSIONS

This work presented an electrification case study in which a backhoe loader is modelled. The power sizing of the main

powertrain components used in the backhoe loader electrification is proposed. The operating cycle called backfill was used in this work. The backfill was detailed and explained. The backhoe loader functioning was introduced. The series hybrid electric topology was the powertrain topology selected and this decision was made based on the backfill characteristics. The traction motor, engine-generator set, and the energy storage source had their powers sized inspired on a technique used for on-road vehicle electrification that was adapted for backhoe loader electrification. The torque, rotating speed and power graphics of the traction motor were obtained. The maximum power value of the traction motor is 82.86 kW. The power sized for the engine-generator set is 19.34 kW. The power and energy values sized for the energy storage source are 78.14 kW and 61.02 kWh respectively.

The backhoe loader model and the power sizing equations were implemented through a script developed in MATLAB. The backhoe loader simulation performed the backfill that demanded high and intermittent peak power values. The simulation showed that the braking kinetic energy recovery does not occur along the backfill due to rolling resistance coefficient and vehicle mass high values. The minimization of power sized for the engine-generator set maximizes the power and energy capacities demanded by the energy storage source. This minimization could hinder the electrification financially.

ACKNOWLEDGMENTS

This work was funded by the research and development foundation – Fundep Rota 2030/Linha V 27192.03.01/2020.15-00.

BIBLIOGRAFY

- Abdel-Baqi, O., Nasiri, A., Miller, P., and Helfrich, J. (2013) Energy System for Heavy Equipment, *US8606451B2*.
- Beutler, A. N., Centurion, J. F., Roque, C. G., & Ferraz, M. V. (2005). Densidade relativa ótima de Latossolos Vermelhos para a produtividade de soja. *Revista Brasileira de Ciência do Solo*, 29, 843-849.
- Cassapa. (2018). Kappa 30 (K30) compact – hydraulic gear pumps and motors.
- Case. (2020). Case 580 EV: First Fully Electric Backhoe. Disponível em: <
<https://www.casece.com/northamerica/en-us/products/backhoe-loaders/580ev-project-zeus>>. Acesso em: 05/04/2022.
- Da Costa, W. *Metodologia Para Conversão de Veículos Equipados Com Motores à Combustão Interna Para Tração Elétrica: Aplicação de Motor Síncrono de Ímã Permanente Com Fluxo Magnético Radial a Um Furgão*. 2009. Dissertação (Mestrado em Engenharia Mecânica) – Faculdade de Engenharia, Universidade Estadual do Rio de Janeiro, Rio de Janeiro.
- Denton, T. (2016). *Electric and hybrid vehicles*. Chapter 4. Routledge. Abingdon

- Ehsani, M., Gao, Y., Longo, S., & Ebrahimi, K. M. (2018). *Modern electric, hybrid electric, and fuel cell vehicles*. Chapter 8. CRC press. Boca Raton.
- Eur-lex. (2016). Document 32016R1628. Disponível em: < <https://eur-lex.europa.eu/eli/reg/2016/1628/oj>>. Acesso em: 08/04/2022.
- Hiroki, T. et al. (2016). Hybrid Construction Machine. *US9290908B2*.
- John Deerer. (2021). John Deere Joint Tests Its First Electric-Powered Backhoe with National Grid. Disponível em: < <https://www.deere.com/en/news/all-news/2021jan06-electric-powered-backhoe/>>. Acesso em: 05/04/2022.
- Kim, D. M., Benoliel, P., Kim, D. K., Lee, T. H., Park, J. W., and Hong, J. P. (2019). Framework development of series hybrid powertrain design for heavy-duty vehicle considering driving conditions. *IEEE Transactions on Vehicular Technology*, 68(7), 6468-6480.
- Liu, X. et al. (2017). Achievement of fuel savings in wheel loader by applying hydrodynamic mechanical power split transmissions. *Energies*, 10(9), p. 1267.
- Liukkonen, M. *Methodologies for development of series-hybrid powertrains to non-road mobile machineries*. 2013. Thesis (Electrical Engineering) - Aalto University, Helsinki.
- Loganathan, M. K., Mishra, B., Tan, C. M., Kongsvik, T., and Rai, R. N. (2021). Multi-Criteria decision making (MCDM) for the selection of Li-Ion batteries used in electric vehicles (EVs). *Materials Today: Proceedings*, 41, 1073-1077.
- Mendes, F. E., Brandao, D. I., Maia, T., & de Filho, J. B. (2019, June). Off-road vehicle hybridization methodology applied to a tractor backhoe loader. *In 2019 IEEE Transportation Electrification Conference and Expo (ITEC)*. pp. 1-6.
- Mi, C., and Masrur, M. A. (2017). *Hybrid electric vehicles: principles and applications with practical perspectives*. Chapter 3. John Wiley & Sons. Chichester.
- O'Keeke, M. P., Simpson, A., and Kelly, K. J. (2007). Duty cycle characterization and evaluation towards heavy hybrid vehicle applications. *SAE World Congress and Exhibition*. pp. 1-12.
- Persistence market research. (2018). Global Market Study on Backhoe Loaders: Significant Demand to be Witnessed in the Agriculture and Forestry Sector During 2017 – 2026. Disponível em: < <https://www.persistencemarketresearch.com/market-research/backhoe-loader-market.asp>>. Acesso em: 05/04/2022.
- Smith, P. F., Prabhu, S. M., & Friedman, J. (2007). Best practices for establishing a model-based design culture. *SAE Technical Paper*. No. 2007-01-0777.
- Stefanow, D. (2018). Experimental determination of selected loading resistance forces of single bucket loader. *24th International Conference engineering mechanics 2018*, pp. 809-812.
- Un-Noor, F., Scora, G., Wu, G., Boriboonsomsin, K., Perugu, H., Collier, S., and Yoon, S. (2021). Operational Feasibility Assessment of Battery Electric Construction Equipment Based on In-Use Activity Data. *Transportation Research Record*, 2675(9), 809-820.
- Wang, H., Huang, Y., Khajepour, A., & Hu, C. (2017). *Electrification of Heavy-Duty Construction Vehicles*. Chapter 2. Morgan & Claypool.
- Wu, C., Kanbayashi, H., & Takanashi, K. (2020). Hybrid Construction Machine. *US10766480B2*.
- Zou, Y., Li, J., Hu, X., & Chamaillard, Y. (2018). *Modeling and Control of Hybrid Propulsion System for Ground Vehicles*. Chapter 8. Springer. Beijing.